Surface structure determination using X-ray standing waves: a simple view

1994 J. Phys.: Condens. Matter 6 10633

(http://iopscience.iop.org/0953-8984/6/49/007)

J. Phys.: Condens. Matter 6 (1994) 10633–10645. Printed in the UK

Surface structure determination using x-ray standing waves: a simple view

D P Woodruff†, B C C Cowie‡ and A R H F Ettema†
† Physics Department, University of Warwick, Coventry CV4 7AL, UK
‡ EPSRC Daresbury Laboratory, Warrington WA4 4AD, UK

Received 6 September 1994

Abstract. In the application of x-ray standing wave (XSW) methods to the determination of surface structures, the experiment provides two structural parameters: the coherent position and the coherent fraction. For simple, single-high-symmetry-site adsorption systems, the interpretation of these parameters in terms of a structural model is trivial, but in the case of lower-symmetry adsorption sites, or multiple adsorption sites (including those associated with coincidence lattice structures), these parameters are related to spatial distribution functions through a Fourier integral. A particularly simple way of viewing this result, in terms of vector (Argand) diagrams, allows many simple cases and general theorems concerning the interconnection of the structure and the XSW fitting parameters to be visualized. The application of this approach is illustrated with particular reference to recent studies of adsorption on FCC (111) metal surfaces, but some generalization to other surfaces is included.

1. Introduction

The quantitative determination of surface structure, and especially of the location of adsorbate species on well-characterized crystal surfaces, is one of the central objectives of many investigations in surface science; knowledge of structure is a key prerequisite for understanding many aspects of the electronic and chemical properties of surfaces. Techniques for investigating surface structure fall broadly into two categories. Diffraction methods, most notably low-energy electron diffraction (LEED) [1,2], but also surface x-ray diffraction [3,4], exploit in a very direct way the two-dimensional long-range order associated with many surface structures, and have proved extremely successful in providing a large part of the existing data-base of 'solved' structures. Other methods, which can rather loosely be described as 'non-diffraction' techniques, such as ion scattering [5,6], surface-extended x-ray absorption fine structure (SEXAFS) [7,8] and photoelectron diffraction [9,10], rely only on local short-range order, and do not specifically exploit the long-range order. Such methods are obviously of especial importance when there is no long-range order in an adsorbate layer, as is commonly the case for molecular adsorbates. A further method that falls into the latter category is x-ray standing-wavefield (XSW) absorption [11,12]; although this technique is specifically based on diffraction in the sub-surface and bulk of a crystal, it does not rely on long-range order in the adsorbate, the location of which is to be determined.

While it is common to distinguish between these diffractive and (essentially) non-diffractive methods in terms of their *requirement* for long-range order in an adsorbate layer, there is another important aspect to this difference. Diffraction methods are well known to *select the long-range ordered part of a surface*, because the diffracted beams are dominated in intensity by these parts of the surface; the scattered intensity from any disordered parts

0953-8984/94/4910633+13$19.50

of the surface is distributed throughout momentum-space and thus contributes relatively little at the diffracted beam locations. This means that if a surface contains regions of good long-range order, and regions of only local order (or complete disorder), a diffraction method will provide unique information on the structure of the long-range-ordered parts alone, whereas the non-diffractive methods will provide some incoherent average of the structure of all parts of the surface. This difference is clearly of some potential importance; the fact that the bulk of our structural data-base still derives from diffraction methods may give us a misleading view of the perfection of surface structures, and indeed over the last few years scanning-probe microscopies have highlighted the relatively poor average quality of many surfaces. One important question that must be addressed by non-diffractive methods is therefore the local structure of parts of the surface that lack long-range order but that coexist with long-range-ordered domains.

In this respect, x-ray standing-wave methods do provide some explicit information on this problem, and this is one of the issues that we address here. More generally, however, it is of interest to understand how the XSW methods combine information from multiple sites, and how the original structural information might be extracted from the results of experimental measurements. The basic mathematics underlying this problem has been presented by other authors over the past 5–10 years of application of the technique (see, e.g., [12–15] and references therein). Some of the simple ideas involved, however, can be obscured by this mathematics, and our object here is to try to present the information in a simple form in order that some general properties can be easily appreciated.

2. Basic theory

In this section we rehearse the basic underlying physics of the XSW experiment, and summarize the mathematical description (which has been derived by others—see, e.g., [12–15]) in a fashion convenient to our later applications. We emphasize in our discussion the normal-incidence XSW (NIXSW) method which we have used in a range of adsorption studies, but remark on the generalization of the main results.

When an x-ray Bragg reflection is established in a crystal, the diffracted wavefield interferes with the incident wavefield to produce a standing wave; the periodicity of the intensity of this standing wave is equal to the spacing of the equivalent scatterer planes (for a first-order diffraction event), and in the simple case of a single diffracted beam and a non-absorbing crystal, we have the classical two-beam interference problem, with the intensity varying spatially between zero and four times that of the incident beam alone ($I_0(1 \pm 1)^2$). A full dynamical analysis of the diffraction [16] which takes account of the attenuation of the incident x-ray wavefield as it penetrates the solid and more flux is removed through backscattering out of the surface, shows that the finite penetration leads to a finite range (and offset) in incidence angle or wavelength, over which total reflectivity is obtained and the standing wave is produced. Within this range, however, the phase of the standing wave shifts in a systematic way relative to the scatterer planes by half the bulk layer spacing. By monitoring the absorption of x-rays by adsorbed atoms (distinguished by their elemental identity) as this standing wavefield shifts, one can deduce the location of the absorber relative to the (extended) bulk scattered planes. This provides the basic measurement of the XSW method; the x-ray absorption at the adsorbate is monitored via photoemission, Auger electron emission or x-ray fluorescence, as the incidence angle or the photon energy is scanned through the nominal Bragg condition.

In the particular variant of the method that we have exploited, the Bragg condition is always excited at (or very close to) normal incidence to the scatterer planes. Under this

condition, the Bragg condition passes through a turning point in its dependence on incidence angle ($2d_H \sin\theta = \lambda$ at $\theta = 90°$) and is therefore insensitive to small variations in incidence angle due to crystal mosaicity, and to limited incident-beam collimation [11, 17]. As such the method is applicable to normal metal single-crystal samples. At more general incidence conditions there is greater flexibility over the x-ray wavelength, but the method is only applicable to very perfect crystals; under these conditions the great majority of surface studies have been performed on silicon [12].

The basic equation governing the experiment is that which defines the intensity of the standing wave at a particular point in space, characterized by a spacing z relative to the extended bulk scatterer planes (which themselves have a periodicity d_H, where the suffix H denotes the indices of the reflection):

$$I = |1 + (E_H/E_0)(\exp(-2\pi i z/d_H))|^2. \tag{1}$$

The amplitude of the electromagnetic scattered wavefield relative to the incident one, E_H/E_0 is just the square root of the reflectivity, R, multiplied by a phase factor, say

$$E_H/E_0 = \sqrt{R}\exp(i\varphi).$$

This means that we can write

$$I = 1 + R + 2\sqrt{R}\cos(\varphi - 2\pi d/D). \tag{2}$$

Note that R and φ are both functions of the photon wavelength (or the incidence angle), and they vary as one sweeps through the Bragg condition to provide the XSW profile.

This analysis is for a single position, so it strictly only applies to an absorber at a single site on a rigid lattice. Suppose, instead, that we have some distribution of possible positions which may be due to vibrational or static disorder, or to several different discrete sites, or both. We can represent this by a distribution of z-values, with a probability of a given value being given by, say, $f(z)\,dz$ within a range dz about the value z. Notice that if this is a proper probability it is normalized such that

$$\int_0^{d_H} f(z)\,dz = 1. \tag{3}$$

In this case, the XSW absorption profile will be given by

$$I = 1 + R + 2\sqrt{R}\int_0^{d_H} f(z)\cos(\varphi - 2\pi z/d_H)\,dz \tag{4}$$

which can also be written as

$$I = 1 + R + 2f_{co}\sqrt{R}\cos(\varphi - 2\pi D/d_H) \tag{5}$$

in terms of two parameters, the *coherent position*, D, and the *coherent fraction* f_{co}. These two parameters totally define the structural dependence of the measured absorption profile, and are thus the parameters that emerge from the analysis of the experimental data.

An alternative way in which equation (5) is often written is

$$I = (1 - f_{co})(1 + R) + f_{co}(1 + R + 2\sqrt{R}\cos(\varphi - 2\pi D/d_H)) \tag{6}$$

which highlights the fact that the absorption profile comprises a coherent part of identical format to that for a single position (equation (2)) attenuated by the factor f_{co}, and an incoherent part which is simply the sum of the incident and reflected beam intensities, multiplied by a factor $1 - f_{co}$.

The equivalence of equations (4) and (5), means that the connection between these measured quantities and the actual spatial distribution function is given by

$$f_{co} \cos(\varphi - 2\pi D/d_H) = \int_0^{d_H} f(z) \cos(\varphi - 2\pi z/d_H)\, dz. \tag{7}$$

This equation tells us that f_{co} is simply the first Fourier component in a Fourier series representation of $f(z)$, but it also contains the coherent position through a phase factor. A more convenient way of representing this information is by using complex numbers. To derive this modification of equation (7), we expand the cosine sums to give

$$\cos\varphi\, f_{co} \cos(2\pi D/d_H) + \sin\varphi\, f_{co} \sin(2\pi D/d_H) = \cos\varphi \int_0^{d_H} f(z) \cos(2\pi z/d_H)\, dz$$
$$+ \sin\varphi \int_0^{d_H} f(z) \sin(2\pi z/d_H)\, dz. \tag{8}$$

As this expression must be true for all values of the phase φ, which varies as one scans through the Bragg condition, and because sine and cosine have opposite parity, this expression can only be satisfied if both the coefficients of $\sin\varphi$ and $\cos\varphi$ can be equated. Thus the two conditions are separated to give

$$f_{co} \cos(2\pi D/d_H) = \int_0^{d_H} f(z) \cos(2\pi z/d_H)\, dz \tag{9a}$$

and

$$f_{co} \sin(2\pi D/d_H) = \int_0^{d_H} f(z) \sin(2\pi z/d_H)\, dz. \tag{9b}$$

An alternative way of writing this condition that both equations (9*a*) and (9*b*) are satisfied is to multiply equation (9*b*) by i (i.e. $\sqrt{-1}$) and to sum the two equations which then become a complex expression for which both real and imaginary parts must be equal. This gives the required alternative form

$$f_{co} \exp(2\pi \mathrm{i} D/d_H) = \int_0^{d_H} f(z) \exp(2\pi \mathrm{i} z/d_H)\, dz. \tag{10}$$

An important attraction of this final formulation is that one can use it to construct a simple graphical representation of the way in which the measured quantities f_{co} and D relate to the integral over a real spatial distribution function. This is achieved using an Argand diagram—each layer spacing in the spatial distribution is represented by a vector, the direction being defined by the phase angle $2\pi z/d_H$ relative to the positive x-axis, while the length is $f(z)$ which is the probability of this value; the resultant (the vector sum of these components) is a vector of length f_{co} and phase angle $2\pi D/d_H$. In the following section we explore some results obtained through this visualization.

3. Some structures and their XSW parameters

3.1. Thermal vibrations and local disorder

One essentially unavoidable deviation, which any real structure must possess relative to the ideal, single-site, rigid-lattice situation that underlies equation (2) (in which the coherent fraction value is implicitly unity), is that there will be thermal vibrations. These actually influence the result in two ways. One is that the vibrations of the substrate scatterers attenuate the diffracted beam intensity by a Debye–Waller factor, and introduce an incoherent component to the standing wavefield itself. This is actually equivalent to reducing the value of f_{co} by this Debye–Waller factor; this bulk lattice contribution is predictable and can be separated out from the unknown spatial distribution function of the absorber atoms. The second influence of thermal vibrations is to introduce a finite width in the adatom distribution function, $f(z)$, which is normally represented by a Gaussian function. Evidently the resulting dephasing of the absorber layer spacing will introduce an incoherent part to the absorption profile which grows as the vibrational amplitude, and thus the Gaussian width, grows. The effects of this through equation (1) can be readily represented on an Argand diagram as seen in figure 1. Notice that, providing the distribution function is symmetrical about its mean position, the resulting coherent position will be unchanged, and only the coherent fraction is affected. If, on the other hand, the distribution is asymmetric, as would result from anharmonic vibrations, then the resultant will be displaced as the distribution broadens. As yet, there appears to have been no experimental observation of this effect, but anharmonicity in adsorbate vibrations at surfaces is likely to be a common phenomena [18].

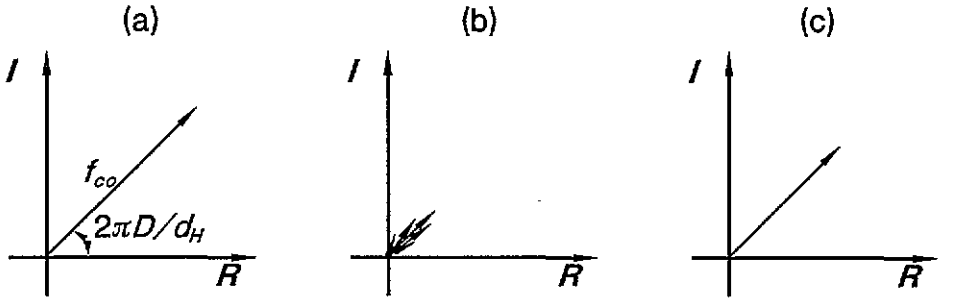

Figure 1. An Argand diagram vector representation of the coherent fraction and coherent position for a single (rigid) adsorption site (a), and for the components (b) and resultant (c) for the same situation with a Gaussian distribution of positions due to thermal vibrations. The real and imaginary axes are marked R and I.

The physical consequence of the influence of harmonic vibrations of the absorbing atoms in XSW is well known, and can be included through a (further) absorber Debye–Waller factor which attenuates f_{co}. The XSW, of course, is only sensitive to the component of the atomic displacement perpendicular to the scatterer planes (which thus leads to variations in z). All of these considerations apply equally to static disorder involving local displacements about some mean positions.

3.2. Two (or more) equally weighted adsorption sites

A second relatively simple case concerns the possible occupation of two distinct adsorption sites on a surface; this may arise because two sites have similar energies, because the adsorbate is adsorbed in two layers, or because one has an adsorbed molecule containing two atoms of the same species that adopt inequivalent sites. The simplest form of this problem is when the two sites have the same probability or weighting. In this case, we must sum the effects of two spacings z_1 and z_2; in the case of a perfect rigid lattice and discrete sites we can attribute individual f-values of their formal weighting, 0.5 to each, and the integral of (10) reduces to a sum of these two values. If we include the effects of local disorder and thermal vibrations, then we have two peaks in the distribution function $f(z)$, but the integral over the full distribution function can be written as a sum of integrals around each peak. If the vibrational and static disorder are the same for both sites, the individual peaks can then each be assigned the same f-values of f_0 which will be the formal weightings (0.5) reduced by the disorder as described in the previous section. In effect, therefore, these f_0 become the weighting multiplied by the value which the coherent fraction would be if only one of these sites was occupied. The resulting XSW profile is then characterized by

$$D = (z_1 + z_2)/2 \qquad f_{co} = f_0 |\cos(\pi(z_1 - z_2)/d_H)|. \tag{11}$$

The general result is thus that the coherent position is just the average of the two layer spacings (figure 2(a)) while the coherent fraction falls as the layer spacing difference increases. This highlights the fact that with a single XSW profile only, one cannot distinguish between a large vibrational amplitude and two distinct layer spacings symmetrically positioned about the same mean layer spacing. (Notice that the simplicity of equation (11) is lost if the two sites have different f_0-values due either to different occupation weightings or to different local disorder.) One particularly interesting consequence of equation (11), however, is that if the two layer spacings differ by $d_H/2$, the resulting coherent fraction is zero! The Argand diagram picture shows this rather graphically (figure 2(b)), because the two vectors are equal and opposite and so cancel in this case. The related mathematical result is that if one samples a pure harmonic function at intervals of half the period, the sum is always equal to the average value of the function; i.e. it is incoherent.

A particularly common case in which there is a need to sum two equally weighted layer spacings in XSW arises for the absorption signal associated with bulk atoms of an elemental crystal having an atomic basis for two atoms. Silicon (and any material having the diamond structure) is such a material. For example, if we consider the (111) reflections from Si, the structure actually comprises double layers of (111) Si planes separated by a quarter of the separation of the 'Bragg planes'; for this reflection therefore, $(z_1 - z_2)/d_H = \frac{1}{4}$, so $f_{co} = 0.71 f_0$. Thus, the bulk (111) reflection from a perfect Si crystal at zero vibrational amplitude would still only give a coherent fraction of 0.71. We should note, however, that in the case of structures having an atomic basis of more than one atom, $D = 0$ need not lie on an atom plane. For the Si(111) case, for example, $D = 0$ lies midway between the double layer of atom planes (passing through the centres of symmetry of the crystal). For a material having an atomic basis of two *inequivalent* atoms, such as the zincblende structure semiconductors (including, for example, GaAs), it is, of course possible to distinguish the two components of the double layers by their elemental identity, but in this case an added complication is that the centres of symmetry are lost and the effective positions of the 'Bragg planes' or 'scattered planes' depend on the individual scattering factors. Indeed, near absorption edges, where the imaginary part of the scattering factors can change strongly,

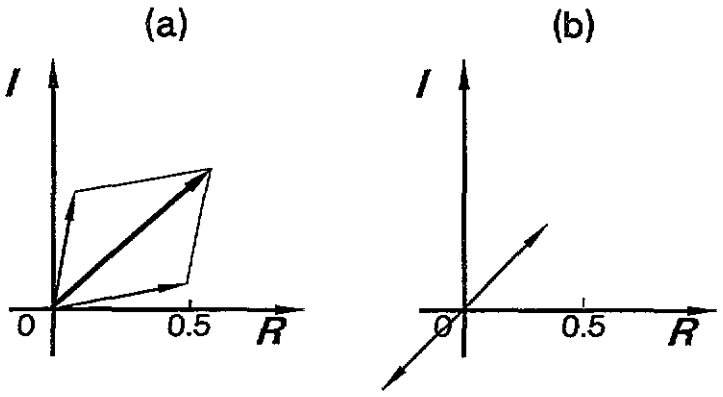

Figure 2. The summation of contributions from two equally weighted layer spacings shown in the Argand diagram representation: (a) shows the components and resultant for the general case; (b) shows the special case of two components with layer spacings differing by half the bulk layer spacing. Both diagrams assume no disorder or vibrations for the individual contributions.

this 'zero' location can be sensitive to the exact photon energy [19]; this complication does not bear, however, on the problem of how to combine different absorber contributions with which we are concerned in this paper.

A further important class of problem in which one may be required to sum over two (or more) equally weighted layer spacings can occur in XSW triangulation experiments. In the application of XSW to the determination of a surface structure, the most obvious experiment (albeit not a totally necessary one) is to set up a reflection from the scattering planes parallel to the surface such that one measures a coherent position, which, in the single-site situation, is simply the layer spacing perpendicular to the surface. In order to determine the adsorption site, however, it is necessary also to measure the layer spacing relative to a second set of scatterer planes that are not parallel to the surface. The combination of the two layer spacings provides the absolute adsorbate site by a simple real-space triangulation [20].

An example of this approach (which is now standard in XSW methodology) is a series of studies that we have conducted on FCC (111) metal surfaces (Cu, Ni, Al) using the (111) reflection (planes parallel to the surface) and the $(\bar{1}\bar{1}1)$ planes (tilted at 70.5° to the surface) (see, e.g., [21–25]). In this case, for a given (111) layer spacing, $D(111)$, one can readily calculate the values of the $(\bar{1}\bar{1}1)$ spacing to be expected from the three possible high-symmetry sites that retain the $3m$ symmetry of the substrate (we will consider lower-symmetry sites in the next section). These sites are atop and the two threefold-coordinated hollows directly above a substrate atom in the second layer ('HCP' hollow) or the third layer ('FCC' hollow). Because these three sites correspond respectively to atop a first-, second- or third-layer substrate atom, and $\cos(70.5°) = \frac{1}{3}$, it is easy to show that the appropriate $(\bar{1}\bar{1}1)$ layer spacings for the three sites are $D(111)/3$, $(D(111) + d(111))/3$, and $(D(111)+2d(111))/3$ (figure 3). Notice that the three associated vectors on an Argand diagram differ in phase by steps of $2\pi/3$, so an equally weighted sum of all three would give a coherent fraction of zero (figure 4(a)). In reality, of course, if all three sites were equally occupied, the atop site would have a larger value of the (111) layer spacing than the hollow sites, so this would not arise. What is perfectly possible, however, is partial (or equal) occupation of both HCP and FCC hollow sites; such a situation is known to occur

in some ordered phases involving more than one adsorbate species per unit mesh (e.g. the c(4 × 2) phase of CO on Ni(111) [26–28]) or at low coverages (e.g. I on Ag(111) [29]). For this double-hollow case, application of equation (11) shows that the ($\bar{1}11$) coherent position would simply be the average of the predicted layer spacings for the two hollows, $(D(111) + 1.5d(111))/3$, and the coherent fraction would be reduced to half of the value expected for exclusive occupation of either site alone (figure 4(b)).

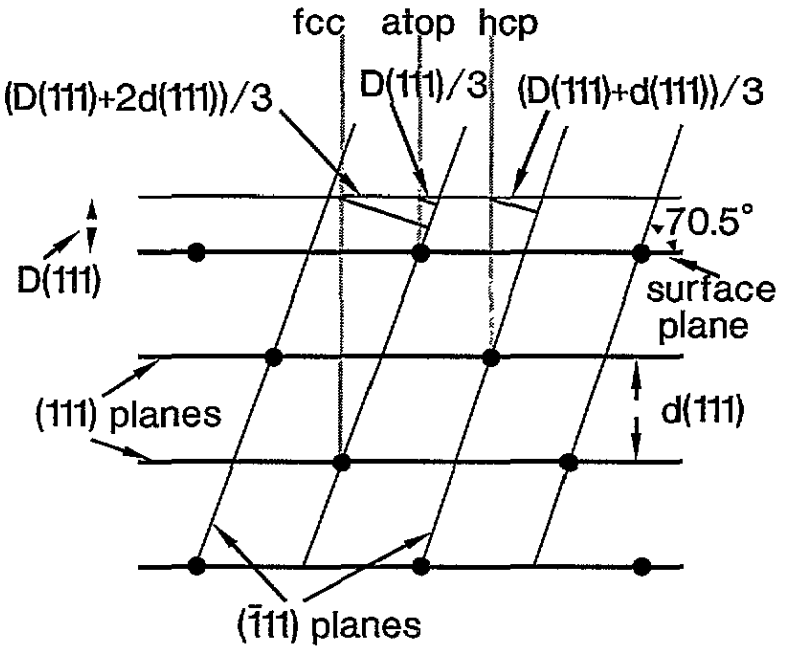

Figure 3. (211) sectional diagram of a FCC (111) crystal surface, showing the relationship of (111) and ($\bar{1}11$) layer spacings for the three fully symmetric adsorption sites.

The cancellation effect of several equally spaced layer spacings is actually a general result of some potential importance. Consider the case of a coincidence lattice (or more properly, a rationally related overlayer mesh) adsorbate structure. In its ideal form such a structure has an adsorbate sub-mesh with a periodicity such that m units of this mesh match n units of the substrate mesh (where m and n are integers). Figure 5(a) shows a two-dimensional illustration of such a structure in which seven overlayer spacings match six substrate spacings. If we now consider any XSW in which the scatterer planes are not parallel to the surface, or parallel to the azimuthal direction of this unit mesh match, the individual layer spacings of the different adsorbate sites will involve regular increments that are rational fractions of the bulk layer spacing for this reflection (in the example of figure 5, these increments are six sevenths of the bulk layer spacing). In such a case, the vector sum over their contributions to the XSW leads to a coherent fraction of zero (figure 5(b)) in exactly the same way as found for the two spacings differing by half a bulk layer spacing, and the three spacings for the ($\bar{1}11$) reflection from a FCC (111) surface with equal numbers of atop, HCP and FCC hollows at the same (111) layer spacing. Of course, in a real coincidence lattice overlayer, we can expect some deviation from the perfect adsorbate sub-mesh via small movements of individual adsorbates parallel and perpendicular to the surface, but we

can still anticipate that the resulting coherent fraction will be low if many inequivalent sites are involved.

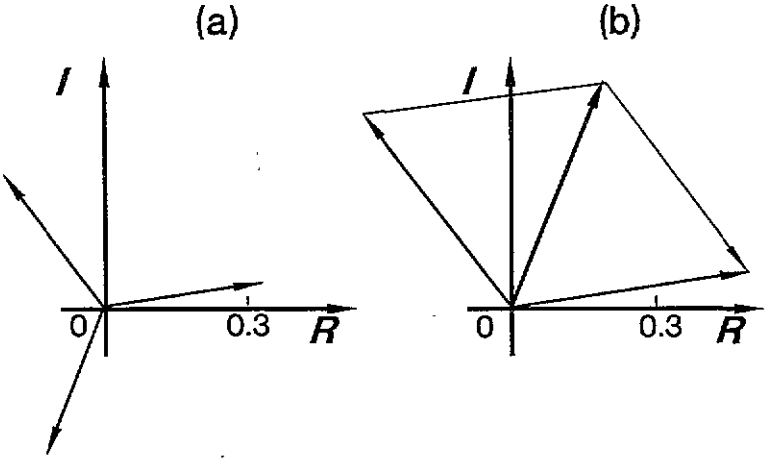

Figure 4. Argand diagram vector representation of the $(\bar{1}11)$ XSW contributions for different combination of mixed adsorption sites on a FCC (111) surface: (a) shows the hypothetical case of equal occupation of all three fully symmetric sites (figure 3) at the same (111) layer spacing; (b) shows the case of equal occupation of HCP and FCC hollows only. The axis scaling assumes perfect order in all sites.

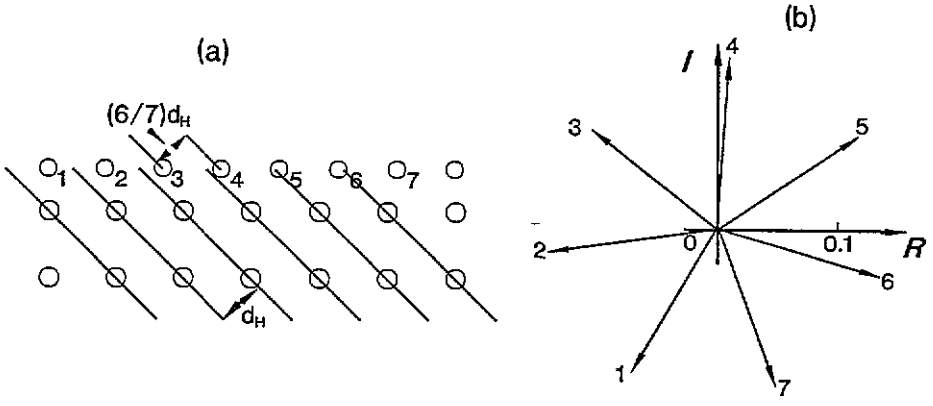

Figure 5. A schematic diagram showing the situation for XSW experiments involving scatterer planes that are not parallel to the surface, in the case of a 'coincidence lattice' or rationally related overlayer case: (a) shows a sectional view of the structure in which seven overlayer spacings match six substrate spacings (note that the overlayer atoms are equally spaced with a period of six sevenths of the bulk layer spacing for this off-normal set of scatterer planes); (b) shows the resulting Argand diagram vector representation of the adsorbate layer components, which exactly cancel. Individual adsorbate atoms within a coincidence unit mesh, and their contributions to the XSW coherent fraction and position, are indicated by the numbers. The *relative* orientations of the contributions do not depend on the adsorbate–substrate registry.

3.3. Low-symmetry adsorption sites and domain averaging

In discussing the problem of adsorption site identification through XSW triangulation in the previous section, the presentation was limited to the case of adsorption sites having the same point group symmetry as the substrate. The reason for this restriction was to avoid the problem of domain structures on surfaces. If the local structure of any surface has a lower point group symmetry than the substrate, it is clear that several different structures must have an equal probability of occurring; these different structures are related by the point group symmetry operations possessed by the substrate but not the surface. The consequence is that we expect the surface to be covered by small domains of these different structures which, on average, will be equally occupied. For example, we expect three inequivalent domains of a rectangular $2m$ surface phase on a $3m$ FCC (111) substrate. From the point of view of XSW, this means that each low-symmetry site on the surface will contribute several z-values to any reflection involving scatterer planes not parallel to the surface.

As an example of this effect, consider again the problem of $(\bar{1}11)$ XSW from adsorbates on an FCC (111) surface. One local site that has a reasonable degree of local symmetry, and is certainly proposed for some adsorbates on these surfaces, is the bridge site midway between two nearest-neighbour surface atoms. This site has only $2m$ symmetry and so there are three inequivalent domains, which actually lead to two different $(\bar{1}11)$ layer spacings; one with a weight of $\frac{1}{3}$ has the value $D(111)/3$ (the same as for an atop site), while the second, with a weight of $\frac{2}{3}$ (corresponding to the other two possible domains), has a value $D(111)/3 + d(111)/2$. These two differ by half the bulk layer spacing, and thus have XSW contributions represented by opposing vectors in the Argand diagram, but the length of the double second is twice that of the first, so the result is a coherent position equal to that of the doubly weighted domain, but with a coherent fraction of a third of the individual values (figure 6). Note that this is a case in which the coherent position is *not* some simple weighted average of the contributing layer spacings (as one might have expected from a generalization of equation (11)).

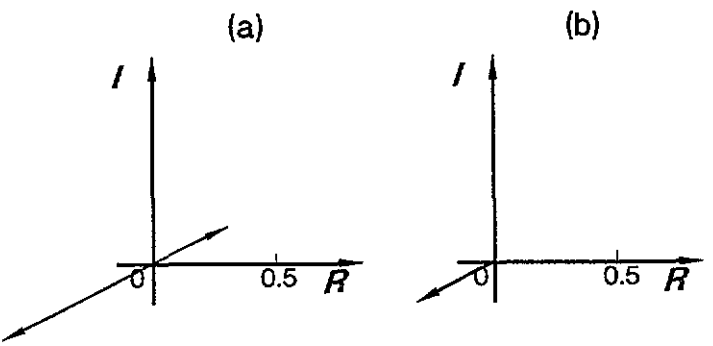

Figure 6. Argand diagram vector representations of the $(\bar{1}11)$ XSW contributions for the three different domains of bridge site on a FCC (111) surface: (a) shows the contributions; (b) shows the resultant. The axis scaling assumes perfect order in all sites.

A further consequence of domain averaging effects for XSW measurements using planes not parallel to the surface is that displacements of atomic locations parallel to the surface away from the high-symmetry sites introduce several inequivalent layer spacings and thus lead to a reduction of coherent fraction. Evidently the exact effect depends on the site, the azimuthal direction of the displacement, and the azimuthal directions of the x-ray scattering

planes, but for small displacements ($\leqslant 0.2$ Å) the effect on the coherent position relative to the ideal high-symmetry site is minimal, and only the coherent fraction is changed (reduced) significantly.

Domain averaging does also impinge on complex surface mesh structures having several inequivalent sites per unit mesh, such as the coincidence lattice structures mentioned in the previous section. In these complex phases, it is often found that local structural techniques (such as SEXAFS) are able to provide some information on the structure within the outer layer (which is often a mixed substrate/adsorbate 'compound' layer), but are less able to establish adsorbate/substrate registry. By contrast, XSW is evidently sensitive only to adsorbate/substrate registry. In the absence of domain effects, one general result highlighted by equation (10) and its vector representation is that for a given adsorbate layer (with fixed relative positions), the coherent fraction of any XSW experiment is independent of the location of this layer relative to the substrate. This result is based on the fact that the relative phases of the component vector contributions from the different adsorbate sites are unchanged by moving the layer rigidly over the surface, and all the vectors rotate by the same amount. The length of the resultant is therefore unchanged. Of course, the direction of the resultant, and thus the coherent position is changed. This simple result is lost, however, as soon as domain averaging is included. Even for a simple overlayer, moving it parallel to the surface moves adsorbate atoms to low-symmetry sites necessitating domain averaging, and in this case the relative phases of the vector contributions from the different phases do change as the layer is moved (indeed, one finds that the contributing vectors from some of the different domains rotate in the opposite sense, an effect that clearly changes both the length and phase (coherent fraction and position) of the resultant). Such effects can therefore only be modelled numerically.

4. General discussion and conclusions

The potential of XSW for structure determination has been recognized for many years, and it has been applied to surface structural problems for almost 15 years. Recognition of the basic significance of the coherent fraction and position resulting from XSW measurements, a necessary prerequisite for the application of the method, is therefore clearly not new. What we have shown here, however, is that by considering the component contributions as vectors on an Argand diagram representation of the Fourier integral of equation (10), many specific and general results relating to the interpretation of these XSW parameters can be obtained in a particularly simple and pictorial fashion. We have identified some examples of the application of this approach, both to specific problems such as double-site occupation and the interpretation of triangulation experiments on FCC (111) surfaces, but also to general problems such as the coincidence lattice structures, the insensitivity of the coherent fraction to the adsorbate–substrate registry for single-domain structures, and the influence of domain averaging. Other applications can be envisaged for the analysis of different problems; for example, a measured coherent fraction and position define the resultant Argand diagram vector, and if one has some specific constraints on the possible structural models (one particular site is partially occupied, or only two sites are occupied), one can understand the range of possible solutions better. We therefore envisage a utility to this approach beyond the specific examples given here.

Some comments may also be in order concerning the problem that we posed in the introduction to this paper, namely the possibility that surfaces apparently yielding good (LEED) diffraction patterns ('having good long-range order') may comprise only a (small)

fraction of long-range-ordered domains with the remainder of the surface being in some sense disordered. Moreover, diffraction methods are not only good at picking out the regions of long-range order, but also picking out *average* long-range order in regions that also contain local defects ('disorder'). Clearly XSW, like all other local structural methods, will provide information that is based on an incoherent average of the different local sites. A clear signature of such multiple sites (if, indeed, the 'disordered' regions do involve different local sites) is a reduction in the coherent fraction, possibly coupled with a change in the coherent position relative to that expected for the long-range-ordered structure. The exact result evidently depends on the nature of the structure of those regions of the surface that lack long-range order.

We envisage three different possibilities for these regions. One is true disorder, in which adsorbed atoms lie in 'random' sites. Such a situation would lead to a constant background to $f(z)$, and thus to a pure incoherent contribution to the resultant XSW absorption profile. One could envisage this true disorder resulting from substrate disorder and distortion (damaged regions, a high density of small-angle grain boundaries etc), but it seems unlikely that it would arise from a sub-monolayer chemisorbed layer on a perfect sub-surface. In this case one would expect well-defined local adsorption sites even in the absence of long-range order in the adsorbate layer. Surface defects (vacancies, steps) would contribute additional sites, but would still correspond to a finite set of distinct sites. A second possibility is that these regions lack long-range order but involve the same local sites as the long-range-ordered domains that give rise to the diffraction pattern. There are many chemisorbed systems in which the local site is thought to be independent of coverage, so this situation may be quite common. The local techniques would then yield essentially the same conclusions concerning the local structure as the diffraction methods (and XSW would see no associated reduction of coherent fraction); all methods would thus be consistent. A third possibility is that the regions that lack long-range order involve different local adsorption sites from the ordered regions, either because of local coverage differences or some other incipient phase transition. In such a situation, local methods can lead to structural conclusions that are quite different from those given by the diffraction techniques; in XSW a lowering of the coherent fraction is a signature of possible multiple sites of this kind. Our recent NIXSW studies of the Al(111) $(\sqrt{3} \times \sqrt{3})$R30°–Rb phases at low and high temperatures [30], compared with data obtained by LEED from a similar study [31], provide an example of such a situation. In such cases XSW may add substantially to our broader understanding of surface structure in a way not accessible to true diffraction methods.

Acknowledgments

We acknowledge the financial support of the EPSRC and the EC (Human Capital and Mobility) in the form of research grants that have allowed this work to proceed.

References

[1] Pendry J B 1974 *Low Energy Electron Diffraction* (New York: Academic)
[2] Van Hove M A, Weinberg W H and Chan C-M 1986 *Low Energy Electron Diffraction, Experiment, Theory and Surface Structure Determination* (Berlin: Springer)
[3] Robinson I K and Tweet D J 1992 *Rep. Prog. Phys.* **55** 599
[4] Feidenhans'l R 1989 *Surf. Sci. Rep.* **10** 105
[5] Niehus H, Heiland W and Taglauer E 1993 *Surf. Sci. Rep.* **17** 213

[6] Van der Veen J F 1985 *Surf. Sci. Rep.* **5** 199
[7] Woodruff D P 1986 *Rep. Prog. Phys.* **49** 683
[8] Stöhr J 1988 *X-ray Absorption: Principles, Applications, Techniques of EXAFS, SEXAFS and XANES* ed D C Koningsberger and R Prins (New York: Wiley) p 443
[9] Woodruff D P and Bradshaw A M 1994 *Rep. Prog. Phys.* at press
[10] Bradshaw A M and Woodruff D P 1994 *Applications of Synchrotron Radiation High-Resolution Studies of Molecules and Molecular Adsorbates on Surfaces* ed W Eberhardt (Berlin: Springer) at press
[11] Woodruff D P, Seymour D L, McConville C F, Riley C F, Crapper M D, Prince N P and Jones R G 1988 *Surf. Sci.* **195** 237
[12] Zegenhagen J 1993 *Surf. Sci.* **18** 199
[13] Hertel N, Materlik G and Zegenhagen J 1985 *Z. Phys.* B **58** 199
[14] Dev B N, Aristov V, Hertel N, Thundat T and Gibson W M 1985 *Surf. Sci.* **163** 457
[15] Herrera'Gómez A, Kendelewicz T, Woicik J C, Miyano K E, Pianetta P, Southworth S, Cowan P L, Karlin A and Spicer W E 1994 *J. Vac. Sci. Technol.* A **12** 2473
[16] Batterman B W 1964 *Phys. Rev.* **133** A749
[17] Woodruff D P, Seymour D L, McConville C F, Riley C F, Crapper M D, Prince N P and Jones R G 1987 *Phys. Rev. Lett.* **58** 1460
[18] Lamble G and King D A 1986 *Phil. Trans. R. Soc.* A **318** 203
[19] Bedzyk M J, Materlik G and Kovalchuk M V 1984 *Phys. Rev.* B **30** 2453
[20] Golovchenko J A, Patel J R, Kaplan D R, Cowan P L and Bedzyk M J 1982 *Phys. Rev. Lett.* **49** 560
[21] Kerkar M, Fisher D, Woodruff D P, Jones R G, Diehl R D and Cowie B 1992 *Phys. Rev. Lett.* **68** 3204
[22] Kerkar M, Hayden A B, Woodruff D P, Kadodwala M and Jones R G 1992 *J. Phys.: Condens. Matter* **4** 5043
[23] Kerkar M, Fisher D, Woodruff D P and Cowie B 1992 *Surf. Sci.* **271** 45
[24] Kerkar M, Woodruff D P, Avila J, Asensio M C, Fernández-Garcia M and Conesa J C 1992 *J. Phys.: Condens. Matter* **4** 6509
[25] Scragg G, Cowie B C, Kerkar M, Woodruff D P, Daïmellah A, Turton S and Jones R G 1994 *J. Phys.: Condens. Matter* **6** 1869
[26] Schindler K-M, Hofman Ph, Weiss K-U, Fritzsche V, Bradshaw A M, Woodruff D P, Davila M, Asensio M C, Conesa J C and González-Elipe A R 1993 *J. Electron. Spectrosc. Relat. Phenom.* **64/65** 75
[27] Mapledoram L D, Wander A and King D A 1993 *Chem. Phys. Lett.* **208** 409
[28] Materer N, Barbiera A, Gardin D, Starke U, Batteas J D, Van Hove M A and Somorjai G A 1993 *Phys. Rev.* B **48** 2859
[29] Farrell H H, Traum M M, Smith N V, Royer W A, Woodruff D P and Johnson P D 1981 *Surf. Sci.* **102** 527
[30] Scragg G, Cowie B C C, Kerkar M, Woodruff D P, Daïmellah A, Turton S and Jones R G 1994 *J. Phys.: Condens. Matter* **6** 1869
[31] Nielsen M, Burchhardt J, Adams D L, Lundgren E and Andersen J 1994 *Phys. Rev. Lett.* **72** 3370